Below-threshold-harmonics-generation limitation due to laser-induced ionization in noble gases

Armando Valter Felicio Zuffi ⑩, Nilson Dias Vieira Junior ⑩, and Ricardo Elgul Samad ⑩[*]

Instituto de Pesquisas Energéticas e Nucleares - IPEN/CNEN, Av. Prof. Lineu Prestes, 2242, 05508-000, São Paulo, SP, Brazil

This work introduces and validates a model that explains an observed upper limitation of the emission of below-threshold harmonics generated by noble gases bound electrons in a restricted region of space. The model uses fundamental parameters from the gases and the laser beam, and correctly predicts an intensity threshold above which the harmonics yield cannot be increased by raising the laser power. This restraint is a consequence from the depletion of electrons due to laser-induced ionization, which exactly compensates the harmonics yield increase with the excitation power.

The efficient generation of ultrashort laser pulses with wavelengths below 300 nm, in the UV range, has been attracting interest due to their use as tools for ultrafast spectroscopy to study femto- and attosecond electronic dynamics in atoms and molecules [1–4], selective ionization [5,6], and other applications [7,8]. Since the 1980s the high-harmonic-generation (HHG) process [9–11], in which atoms in a gas are ionized and the freed electrons emit harmonics upon recombination, has dominated this landscape, but in the last decade below-threshold harmonics (BTH) have been receiving attention [12–14]. The BTH are also generated in gases, by bound electrons that respond nonlinearly to the laser-field frequency, oscillating at its odd harmonics [15] in the perturbative and nonperturbative regimes [16]. This constraint, that keeps the electrons tied to their atoms, limits the BTH photon energy to below the first ionizing energy of the atom to wavelengths usually longer than ∼100 nm. Additionally, the nth harmonic intensity is proportional to the nth power of the laser intensity due to the predominant perturbative character of its generation [15].

BTH have been used in ultrafast spectroscopy [13,14], in frequency comb technology for precision measurements [17,18], and to boost the efficiency in high-order harmonic generation [19]. Besides that, Yost *et al.* [17] initiated an intense investigation activity on the BTH underlying mechanisms, mostly for harmonics close to the ionization threshold, which present a transition from the perturbative [15] to the nonperturbative regime [16,20–22].

The BTH generation depends on the gas medium nonlinear properties, and noble gases constitute the simplest systems for this end for being monoatomic, also emitting the shortest wavelengths down to 50.4 nm for helium (highest ionizing energy in gases, at 24.6 eV). A requirement to generate harmonics in the vacuum ultraviolet (VUV) range is to work inside a vacuum chamber since atmospheric molecular oxygen strongly absorbs wavelengths below ∼250 nm (and molecular nitrogen below ∼150 nm), and, also, to restrict

the gas to the laser focus region where the harmonics are generated, preventing energy loss by interaction with the surrounding media. Additionally, efficient harmonic generation in noble gases requires laser intensities of about TW/cm² due to the small nonlinear susceptibilities of these atoms, and the proper pressure ranges. Furthermore, BTH presents an strong decrease of the harmonic yield with growing harmonic order [15], demanding high laser intensities, close to the ionization threshold.

This paper presents an experimental study of BTH generation in noble gases, in which a capping of the harmonics emission was observed in the lower ionizing energy gases, and proposes a simplified model based on the geometry of the harmonics generation region to explain this upper limiting as a function of fundamental parameters.

BTH were generated in four noble gases (krypton, argon, neon, and helium) by ultrashort laser pulses from a Ti:sapphire chirped pulse amplification (CPA) laser system (Femtolasers Femtopower Compact Pro HR/HP). The laser pulses are centered at 785 nm with 35 nm of bandwidth (full width at half maximum, FWHM), energy up to 550 μJ, at 4-kHz repetition rate, in a laser beam with $M^2 < 1.5$. This CPA system has a prism compressor, and the pulses duration can be controlled by adjusting the prisms distance, from 200 fs to a minimum of 25 fs (FWHM).

The harmonics generation occurs inside a cylindrical vacuum chamber with a gas line coupled to a nozzle [23]. The vacuum is made by a turbomolecular pump resulting in final background pressures below 10^{-6} mbar. To generate the harmonics, the laser beam is focused by an external planoconvex lens ($f = 50$ cm) into the gas nozzle inside the vacuum chamber, to a 35-μm beamwaist [23], reaching intensities above 5×10^{14} W/cm² for the shortest pulses (25 fs). The noble gas flows through the nozzle at a 100-mbar constant pressure inside it. The nozzle consists of a 2.3-mm inner diameter glass capillary etched with ultrashort pulses in a homemade machining system to reduce its wall thickness to 200 μm, so it can be drilled by the same beam that generates the harmonics [24]. This defines an interaction length $\ell = 2.7$ mm (assuming that the gas pressure drops abruptly outside the nozzle), which
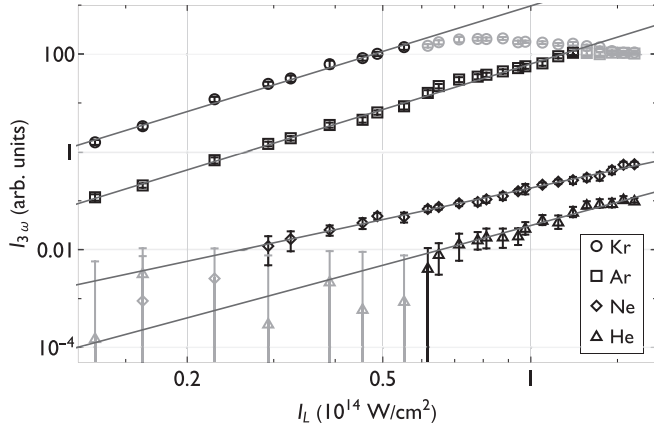
─────────
[*]resamad@ipen.br

FIG. 1. Third-harmonic yield for noble gases and fitted power functions.

provides good phase-matching conditions for the generation of up to the seventh harmonic in argon [25].

The harmonics were measured by a VUV monochromator (McPherson 234/302), which covers the spectral range from 30 to 300 nm and has a 200-mm focal length concave holographic diffraction grating, aperture $f/4.5$, and resolution of 1 Å at 584 Å. The detection is made by a photomultiplier tube with a scintillator coated with sodium salicylate, and its signal is analyzed by a lock-in amplifier and stored on a computer. Care was taken to ensure that the experimental response was always linear with the harmonic-generated intensity, independently of the gas used. In the results presented here the nth harmonic intensity (yield), $I_{n\omega}$, is its peak intensity [23].

Figure 1 presents the third-harmonic yield, $I_{3\omega}$, as a function of the laser pulses intensity, I_L, for 40-fs pulses, for the four noble gases, and data fittings to each gas dataset by a simple power function:

$$I_{3\omega} = A I_L^p, \tag{1}$$

where A is the amplitude of the fit, which indicates the harmonic-generation strength, and p is the order of the harmonic-generation process. The points that strongly deviated from the power behavior given by (1), indicated by faded symbols in the graph, were not considered for the fittings. These points are the lowest-intensity ones for neon and helium, for which the weak harmonic intensity is on the order of the instrumental noise, and the highest-intensity ones for krypton and argon, where a saturation can be observed. The fittings parameters for each gas are shown in the last two columns of Table I, along with the two initial ionization energies (E_{ion}) and corresponding ionization intensity thresholds (I_{th}). These I_{th} values are given by a simple model [26,27] that assumes that the ionization occurs by Coulomb-barrier suppression, and that all atoms subjected to intensities I_{th} and above lose their valence electrons.

The fitting exponents p present values close to 3, confirming that the harmonic-originating nonlinearity is a perturbative third-order process, characteristic of bound electrons. The fitting amplitude (harmonic-generation strength), A, decreases as the gas first ionization energy grows, and their plotting in a log scale, as shown in Fig. 2, reveals that the

TABLE I. Noble gases ionization parameters and fitting parameters for the third-harmonic response.

Gas	First ionization E_{ion} (eV)	First ionization I_{th} (10^{14}W/cm^2)	Second ionization E_{ion} (eV)	Second ionization I_{th} (10^{14}W/cm^2)	A	p
Kr	14.00	1.5	24.36	3.5	964(92)	3.09(8)
Ar	15.76	2.4	27.63	5.8	63(2)	3.10(5)
Ne	21.57	8.7	40.96	28	0.183(3)	2.14(5)
He	24.59	15	54.42	88	0.031(2)	2.7(2)

harmonic-generation strength falls exponentially, dropping approximately by 1 order of magnitude for each 2-eV increase in the ionization energy. This efficiency decrease can be qualitatively explained by a simple model that considers that the valence electron is bound to the atom by a spring (Hooke-type force) whose constant grows with the ionization energy. This is justified considering that, as E_{ion} increases, a stronger force is needed to displace the electron from its equilibrium position, resulting in a smaller amplitude oscillation when compared to a lower ionization energy bound electron. This also results in smaller oscillations at higher frequencies (harmonics) when a nonlinear response is present.

To investigate the third-harmonic deviation from the power law at high intensities, observed in krypton and argon in Fig. 1, the third-harmonic yield dependence on the laser intensity was measured in argon for constant pulse energy and varying pulse duration. This procedure was adopted to take advantage of the fact that the pulse duration can be quickly changed by tuning the CPA compressor, and the measurement can be done in a short time, minimizing the effect of power fluctuations. Moreover, the measurement can be done for different pulse energies, to verify if the saturation has a dependence on other parameter besides the pulse intensity. The results obtained for three pulse energies (350, 425, and 525 μJ), and pulse durations ranging from 25 to 200 fs, are presented in Fig. 3. The third-harmonic yield is almost the same for the three pulse energies, increasing very closely to the third power of the laser intensity (I_L^3, dashed line) up to
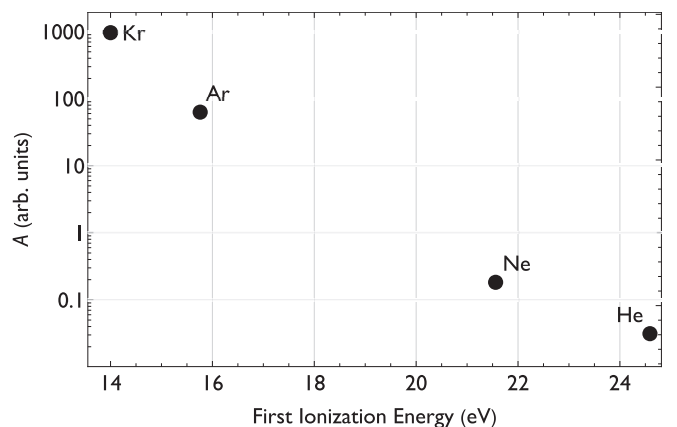

FIG. 2. Amplitude (harmonic-generation strength) of the third-harmonic dependence on the gas first ionization energy.
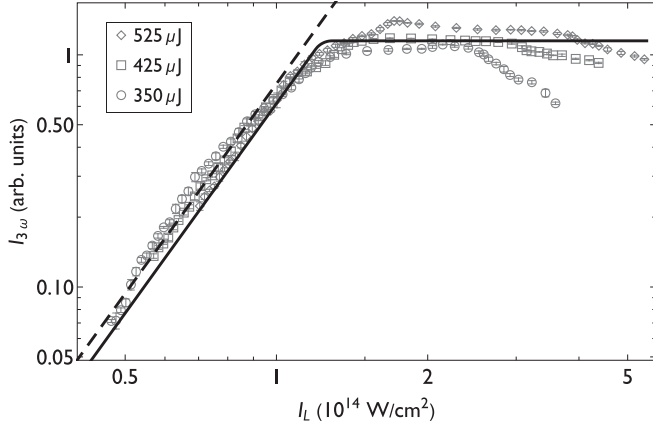
FIG. 3. Third-harmonic yield in argon dependence on the pulse intensity, for different pulse energies. The dashed line is proportional to the third power of the laser intensity, and the continuous line is the result of the numerical integration of Eq. (5).

$I_L \approx 1.4 \times 10^{14}\,\mathrm{W/cm^2}$, when a plateau is stablished slightly above 1. As the laser intensity increases, the yield drops from the plateau level at different intensities for each pulse energy.

To describe the plateau, we hypothesized that the harmonic-yield drop results from ionization that depletes the valence bound electrons that generate the third harmonic. This can occur since the laser peak intensities are close to the barrier suppression ionization (BSI) threshold for the first ionization of argon, given in Table I, and when this threshold is exceeded all the atoms subjected to this intensity (and higher) are ionized [26,27]. Ganeev *et al.* [28] proposed this mechanism as responsible for the occurrence of a saturation, and here we provide a mathematical treatment to validate this process. After ionization, the new valence electron has a much higher ionization energy (second ionization energy, Table I), and according to Fig. 2, as E_{ion} increases, the harmonic strength decreases; therefore, although the new valence electron (second electron of the neutral atom) oscillates in the laser field and emits the third harmonic, its yield is much smaller than that of the neutral atom first electron, not contributing noticeably to the harmonic intensity. For argon, we estimate, based on Fig. 2 and Table I, that the second electron harmonic yield is $< 10^{-4}$ of the first electron output.

Assuming, without loss of generality, that the third harmonic is generated for intensities above a threshold $I_{3\omega\_th}$, when an ultrashort pulse is focused in a gas, only those atoms inside the isointensity surface defined by $I_{3\omega\_th}$ will generate the harmonic. For a transverse electromagnetic mode TEM$_{00}$ Gaussian beam propagating in the z direction and focused at the origin, the radius $\rho(z, I_{3\omega\_th})$ of this isointensity surface is given by [29]

$$\rho(z,\, I_{3\omega\_th}) = \sqrt{\frac{w(z)^2}{2}\ln\left(\frac{2}{\pi\,w(z)^2}\frac{P_0}{I_{3\omega\_th}}\right)}, \qquad (2)$$

where P_0 is the pulse power and $w(z)$ is the laser spot-size radius:

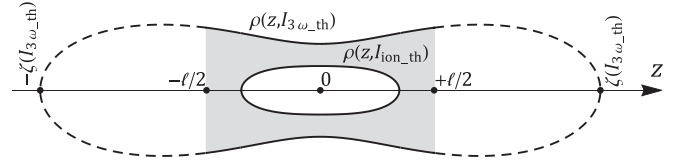$$w(z) = w_0\left(1 + \left(\frac{z}{z_R}\right)^2\right)^{1/2}, \qquad (3)$$

with w_0 being the focused pulse beamwaist, and $z_R = (\pi\,w_0^2)/\lambda$ the beam Rayleigh range, where λ is the laser wavelength. The volume defined by this isointensity surface has the shape of a cigar for low laser intensities, and as the intensity grows it changes to a dumbbell when above a critical power [29]. The limits of this surface in the z axis are $\pm\zeta(I_{3\omega\_th})$, where [29]

$$\zeta(I_{3\omega\_th}) = \frac{\pi w_0^2}{\lambda}\left(2\frac{I_0}{I_{3\omega\_th}} - 1\right)^{1/2}, \qquad (4)$$

which grows as the pulse power increases, with $I_0 = P_0/(\pi\,w_0^2)$ being the laser intensity at the focus.

When focusing the pulses on the middle of a gas region with length ℓ (interaction length) and no transversal limitation, the third harmonic will be generated inside the volume enclosed by the isointensity surface given by $\rho(z, I_{3\omega\_th})$. For low pulse powers, the length of this region will be $2\zeta(I_{3\omega\_th})$ when $\zeta(I_{3\omega\_th}) < \ell/2$; as the pulse power increases, this extent grows and becomes limited to ℓ when $\zeta(I_{3\omega\_th}) > \ell/2$, as indicated in Fig. 4. The third-harmonic total yield, $I_{3\omega}$, will be proportional to the third power of the intensity integrated over the volume limited by $\rho(z, I_{3\omega\_th})$, but it will be reduced if atoms are ionized, which will occur inside an isointensity surface limited by the BSI threshold, I_{ion_th}. These two isointensity surfaces define the shadowed region in Fig. 4 that generates the third harmonic, which will be a ring when both surfaces are longer than ℓ. With these considerations, the third-harmonic yield can be written as

$$(I_{3\omega})^{1/3} = \alpha\int_{-\ell/2}^{\ell/2} dz\int_{\rho(z,\,I_{ion\_th})}^{\rho(z,\,I_{3\omega\_th})} dr\int_0^{2\pi} r\,d\theta\,\frac{2P_0}{\pi\,w(z)^2}$$
$$\times\,\exp\left\{-2\frac{r^2}{w(z)^2}\right\}, \qquad (5)$$

where α is a proportionality constant related to the nonlinear process that generates the third harmonic, and the last term is the laser intensity density in cylindrical coordinates for a pulse with power P_0 [29]. The last integral is 2π due to the beam cylindrical symmetry, and the limits of the first integral, $[-\ell/2,\, \ell/2]$, assume a gas region with length ℓ with the laser beam focused at its center, generating isointensity surfaces that are symmetrical around the origin, as represented in Fig. 4. The second integral, in the radial direction, runs from the internal isointensity surface defined by the gas ionization threshold, $\rho(z, I_{ion\_th})$, up to the external surface defined

FIG. 4. Representation of the radius of the third harmonic, $\rho(z, I_{3\omega\_th})$, and ionization, $\rho(z, I_{ion\_th})$, thresholds isointensity surfaces, and the region with gas (shadowed), in which the third harmonic is generated. The dashed lines indicate the region in which no harmonic is generated due to gas absence.

by the third-harmonic-generation threshold, $\rho(z, I_{3\omega\_th})$, summing all the third-harmonic contribution from the shadowed region in Fig. 4.

The radial exponential integral in Eq. (5), and the resulting longitudinal integral have primitives and can be easily calculated. However, since the harmonic generation and the ionization regions lengths increase and get longer than the gas region as the laser intensity rises, the integral has to be broken into several domains: the first one occurs when there is no ionization and the harmonic isointensity surface is shorter than the gas region, and in this case the second integral goes from zero to $\rho(z, I_{3\omega\_th})$ and the first one covers all its length; as the intensity increases, the harmonic-generation volume becomes longer than the gas region, and the first integral limits are $-\ell/2$ and $\ell/2$; for higher yet intensities, ionization starts to occur and its volume increases, eventually becoming longer than the gas region, and the first and second integrals have to be solved for different sets of limits. For these reasons, to investigate the third-harmonic yield as the pulse intensity goes from zero to higher than the one at which both isointensity surfaces became longer than the gas region length, numerical integration is better suited.

The integral in Eq. (5) was numerically calculated for the argon first ionization threshold (Table I), the experimental parameters, and $I_{3\omega\_th} = 0$. This value agrees with perturbative processes, which occur even for intensities close to zero, with negligible contribution. The integration result is shown as the continuous line in Fig. 3. The agreement between the experimental data and the numerical integration is very good, especially considering that the continuous curve is not a fit: the only free parameter in Eq. (5) is α, which takes into account the harmonic-generation process and the instrumental efficiency, and was adjusted to match the experimental data. The theoretical curve describes the third-harmonic increase with the laser intensity and the existence of the plateau, giving a good prediction of the laser intensity at which it is established. The discrepancies between the experimental data and the numerical curve probably arise from the beam being not perfectly Gaussian and the gas not having sharp boundaries in the z direction, creating deviations in the isointensity surfaces, and also from the pulse chirp which can modify the harmonic generation and ionization mechanisms. For the highest intensities, the plateau drops, and this is likely due to the onset of competing nonlinear processes that divert excitation energy from the third-harmonic generation, and plasma formation that impairs phase matching, which are not considered in the presented model.

By analytically integrating Eq. (5), it can be shown that the plateau is reached when $\zeta(I_{ion\_th}) = \ell/2$, i.e., the length of the isointensity surface defined by the gas ionization threshold is equal to the length of the gas region, and solving this condition for the pulse intensity provides I_{p_th}, the laser intensity threshold at which the plateau is established:

$$I_{p\_th} = \frac{I_{ion\_th}}{2}\left(1 + \frac{\ell^2}{b^2}\right), \qquad (6)$$

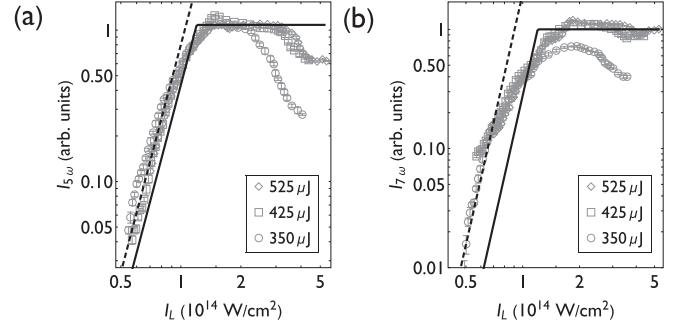where $b = 2z_R$ is the beam confocal parameter. Applying Eq. (6) with our experimental parameters

FIG. 5. (a) Fifth- and (b) seventh-harmonic yields in argon as a function of the laser intensity.

($w_0 = 35\,\mu$m, $\ell = 2.7$ mm, $\lambda = 785$ nm) to the first ionization intensities of the used gases provides $I_{p\_th}(\text{Kr}) = 0.8 \times 10^{14}$ W/cm^2, $I_{p\_th}(\text{Ar}) = 1.3 \times 10^{14}$ W/cm^2, $I_{p\_th}(\text{Ne}) = 4.7 \times 10^{14}$ W/cm^2, and $I_{p\_th}(\text{He}) = 8.1 \times 10^{14}$ W/cm^2. The values for krypton and argon agree well with the data shown in Fig. 1, and also explain that the plateau did not appear for neon and helium because we could not reach their threshold intensities.

The analytical integration also provides the plateau value:

$$I_{plat} = \alpha^3\left(\frac{(I_{ion\_th} - I_{3\omega\_th})(\ell^3\lambda^2 + 12\pi^2 w_0^4 \ell)}{24\pi w_0^2}\right)^3. \qquad (7)$$

When the intensity threshold I_{p_th} is reached the harmonic yield is capped at I_{plat}, and increasing the laser power results in no augmentation of the harmonic yield, and raising its output demands changing the parameters in Eq. (7); the most effective way to do this is increasing the interaction length, which provides an $\sim\ell^9$ gain in the harmonic yield (as long as the phase-matching condition is kept [25]). Considering only Eq. (7), changing the gas by one with a higher ionization threshold should enhance the harmonic yield by $\sim I_{ion\_th}^3$, since the ionized gas volume would become smaller. However, results presented in Fig. 2 evidence that in this case the harmonic-generation strength would decrease exponentially (α contains the nonlinear susceptibility, which causes this decline), effectively reducing the harmonic yield. Therefore, contrary to Eq. (7), to experimentally increase the harmonic intensity demands using a lower ionization threshold gas.

The intensity threshold given in Eq. (6) is valid for any bound electron effect generated in a restricted region in a gas, particularly for BTH, and depends only on the ionization threshold. The intensity of the nth harmonic response curve is given by the nth power of the integral in Eq. (5) with the appropriate intensity thresholds. Figure 5 shows the validity of this prediction for the fifth- [Fig. 5(a)] and seventh- [Fig. 5(b)] harmonics generated in argon for the same previous experimental conditions, also confirming Eq. (6) result that the laser intensity at which the plateau is established does not depend on the effect order, only on the gas ionization threshold value. The slope discrepancy for the seventh harmonic is probably due to an efficiency decrease from bad phase matching [25], low signal amplitude, and nonperturbative behaviors such as

HHG [30] that have stronger influence on perturbative harmonics closer to the ionization edge.

In conclusion, we proposed and validated a model that predicts the existence of a plateau for the response of bound electrons effects arising from a gas in a restricted region of space. The plateau comes from a geometric consideration that takes into account the depletion of electrons by ionization, and the negligible contribution from the second valence electrons due to their higher ionizing energy. After the plateau is reached, as the laser intensity rises, the harmonic yield increases according to Eq. (1) and the generating volume growth, but this is exactly compensated by the electrons depletion (ionization close to the propagation axis). This is an unexpected result because, intuitively, there should be no limitation for the harmonic yield, and this restriction comes from solving the integral in Eq. (5).

We expect that the intensity threshold derived here for the bound electrons depletion in a restricted region of matter can be applied for a variety of perturbative effects beyond the direct harmonic generation, such as wave mixing, cascaded harmonic generation, and Kerr effect, among others.

All authors contributed equally for the theoretical model development. A.V.F. Z. conducted the experiments.

[1] A. L. Cavalieri *et al.*, Attosecond spectroscopy in condensed matter, Nature (London) **449**, 1029 (2007).

[2] M. Chini *et al.*, Coherent phase-matched VUV generation by field-controlled bound states, Nat. Photonics **8**, 437 (2014).

[3] P. C. Li, Y. L. Sheu, C. Laughlin, and S. I. Chu, Role of laser-driven electron-multirescattering in resonance-enhanced below-threshold harmonic generation in He atoms, Phys. Rev. A **90**, 041401 (2014).

[4] Y. Nabekawa, Y. Furukawa, T. Okino, A. A. Eilanlou, E. J. Takahashi, K. Yamanouchi, and K. Midorikawa, Sub-10-fs control of dissociation pathways in the hydrogen molecular ion with a few-pulse attosecond pulse train, Nat. Commun. **7**, 12835 (2016).

[5] H. Rottke and K. H. Welge, State-selective resonant excitation-ionization of H_2 with tunable VUV laser light, Chem. Phys. Lett. **99**, 456 (1983).

[6] J. Y. Feng, Y. P. Lee, H. A. Witek, and T. Ebata, Vacuum ultraviolet photoionization induced proton migration and formation of a new C-N bond in pyridine clusters revealed by infrared spectroscopy and mass spectrometry, J. Phys. Chem. Lett. **12**, 4936 (2021).

[7] A. Ozawa and Y. Kobayashi, vuv frequency-comb spectroscopy of atomic xenon, Phys. Rev. A **87**, 022507 (2013).

[8] J. Reichert, M. Niering, R. Holzwarth, M. Weitz, T. Udem, and T. W. Hansch, Phase Coherent Vacuum-Ultraviolet to Radio Frequency Comparison with a Mode-Locked Laser, Phys. Rev. Lett. **84**, 3232 (2000).

[9] A. Mcpherson, G. Gibson, H. Jara, U. Johann, T. S. Luk, I. A. Mcintyre, K. Boyer, and C. K. Rhodes, Studies of multiphoton production of vacuum ultraviolet-radiation in the rare-gases, J. Opt. Soc. Am. B **4**, 595 (1987).

[10] R. A. Bartels, A. Paul, H. Green, H. C. Kapteyn, M. M. Murnane, S. Backus, I. P. Christov, Y. Liu, D. Attwood, and C. Jacobsen, Generation of spatially coherent light at extreme ultraviolet wavelengths, Science **297**, 376 (2002).

[11] J. Rutledge, A. Catanese, D. D. Hickstein, S. A. Diddams, T. K. Allison, and A. S. Kowligy, Broadband ultraviolet-visible frequency combs from cascaded high-harmonic generation in quasi-phase-matched waveguides, J. Opt. Soc. Am. B **38**, 2252 (2021).

[12] A. Cingoz, D. C. Yost, T. K. Allison, A. Ruehl, M. E. Fermann, I. Hartl, and J. Ye, Direct frequency comb spectroscopy in the extreme ultraviolet, Nature (London) **482**, 68 (2012).

[13] J. Heslar, D. A. Telnov, and S. I. Chu, Enhancement of VUV and EUV generation by field-controlled resonance structures of diatomic molecules, Phys. Rev. A **93**, 063401 (2016).

[14] L. N. Li, J. P. Wang, and F. He, Roles of Coulomb potentials in below- and above-threshold harmonic generation for a hydrogen atom in strong laser fields, J. Opt. Soc. Am. B **33**, 1558 (2016).

[15] R. W. Boyd, *Nonlinear Optics*, 2nd ed. (Academic, San Diego, 2003).

[16] A. Spott, A. Becker, and A. Jaron-Becker, Transition from perturbative to nonperturbative interaction in low-order-harmonic generation, Phys. Rev. A **91**, 023402 (2015).

[17] D. C. Yost, T. R. Schibli, J. Ye, J. L. Tate, J. Hostetter, M. B. Gaarde, and K. J. Schafer, Vacuum-ultraviolet frequency combs from below-threshold harmonics, Nat. Phys. **5**, 815 (2009).

[18] C. Benko, T. K. Allison, A. Cingoz, L. Q. Hua, F. Labaye, D. C. Yost, and J. Ye, Extreme ultraviolet radiation with coherence time greater than 1 s, Nat. Photonics **8**, 530 (2014).

[19] F. Brizuela, C. M. Heyl, P. Rudawski, D. Kroon, L. Rading, J. M. Dahlstrom, J. Mauritsson, P. Johnsson, C. L. Arnold, and A. L'Huillier, Efficient high-order harmonic generation boosted by below-threshold harmonics, Sci. Rep. **3**, 1410 (2013).

[20] J. K. Wahlstrand, S. Zahedpour, A. Bahl, M. Kolesik, and H. M. Milchberg, Bound-Electron Nonlinearity Beyond the Ionization Threshold, Phys. Rev. Lett. **120**, 183901 (2018).

[21] W. H. Xiong, J. W. Geng, J. Y. Tang, L. Y. Peng, and Q. H. Gong, Mechanisms of Below-Threshold Harmonic Generation in Atoms, Phys. Rev. Lett. **112**, 233001 (2014).

[22] H. Soifer, P. Botheron, D. Shafir, A. Diner, O. Raz, B. D. Bruner, Y. Mairesse, B. Pons, and N. Dudovich, Near-Threshold High-Order Harmonic Spectroscopy with Aligned Molecules, Phys. Rev. Lett. **105**, 143904 (2010).

[23] A. V. F. Zuffi, A. A. Almeida, N. D. Viera, and R. E. Samad, Characterization of below threshold harmonics generated in argon by ultrashort laser pulses, in *2018 SBFoton International Optics and Photonics Conference (SBFoton IOPC)* (IEEE, New York, 2018).

[24] A. V. F. Zuffi, A. A. Almeida, N. D. Vieira, and R. E. Samad, Development of glass nozzles for below threshold harmonics and high harmonic generation, in *Frontiers in Optics + Laser Science APS/DLS* (Optical Society of America, Washington, DC, 2019), JTu3A.44.

[25] A. V. F. Zuffi, A. A. Almeida, N. D. Viera, and R. E. Samad, Below threshold harmonics dependence with phase-matching parameters in argon, in *2019 SBFoton International Optics and Photonics Conference (SBFoton IOPC)*, (IEEE, New York, 2019).

[26] S. Augst, D. Strickland, D. D. Meyerhofer, S. L. Chin, and J. H. Eberly, Tunneling Ionization of Noble-Gases in a High-Intensity Laser Field, Phys. Rev. Lett. **63**, 2212 (1989).

[27] S. Augst, D. D. Meyerhofer, D. Strickland, and S. L. Chin, Laser ionization of noble-gases by Coulomb-barrier suppression, J. Opt. Soc. Am. B **8**, 858 (1991).

[28] R. A. Ganeev, G. S. Boltaev, R. I. Tugushev, T. Usmanov, M. Baba, and H. Kuroda, Third harmonic generation in plasma plumes using picosecond and femtosecond laser pulses, J. Opt. **12**, 055202 (2010).

[29] R. E. Samad and N. D. Vieira, Geometrical method for determining the surface damage threshold for femtosecond laser pulses, Laser Phys. **16**, 336 (2006).

[30] C. Wahlstrom, J. Larsson, A. Persson, T. Starczewski, S. Svanberg, P. Salieres, P. Balcou, and A. L'Huillier, High-order harmonic generation in rare gases with an intense short-pulse laser, Phys. Rev. A **48**, 4709 (1993).